Author/s:
McGuigan, S;Pelentritou, A;Scott, DA;Sleigh, J

Title:
Xenon anaesthesia is associated with a reduction in frontal electroencephalogram peak alpha frequency

Date:
2024-12

Citation:
McGuigan, S., Pelentritou, A., Scott, D. A. & Sleigh, J. (2024). Xenon anaesthesia is associated with a reduction in frontal electroencephalogram peak alpha frequency. BJA Open, 12, https://doi.org/10.1016/j.bjao.2024.100358.

Persistent Link:
https://hdl.handle.net/11343/359320

BJA Open

BJA Open, 12 (C): 100358 (2024)

doi: 10.1016/j.bjao.2024.100358
Original Research Article

ORIGINAL RESEARCH ARTICLE

Xenon anaesthesia is associated with a reduction in frontal electroencephalogram peak alpha frequency

Steven McGuigan[1,2,*], Andria Pelentritou[3], David A. Scott[1,2] and Jamie Sleigh[4]

[1]Department of Anaesthesia and Acute Pain Medicine, St. Vincent's Hospital, Melbourne, VIC, Australia, [2]Department of Critical Care, University of Melbourne, Melbourne, VIC, Australia, [3]Department of Clinical Neurosciences, Lausanne University Hospital and the University of Lausanne, Lausanne, Switzerland and [4]Department of Anaesthesia, Waikato Clinical School, Waikato Hospital, University of Auckland, New Zealand

*Corresponding author. Department of Anaesthesia and Acute Pain Medicine, St. Vincent's Hospital, Melbourne, VIC, Australia. E-mail: steven.mcguigan@svha.org.au

Abstract

Background: Administration of conventional anaesthetic agents is associated with changes in electroencephalogram (EEG) oscillatory dynamics, including a reduction in the peak alpha frequency. Computational models of neurones can reproduce such phenomena and are valuable tools for investigating their underlying mechanisms. We hypothesised that EEG data acquired during xenon anaesthesia in humans would show similar changes in peak alpha frequency and that computational neuronal models of recognised cellular actions of xenon would be consistent with the observed changes.
Methods: EEG recordings were obtained for 11 participants from a randomised controlled trial of xenon anaesthesia and for 21 participants from a volunteer study of xenon administration. The frontal peak alpha frequency was calculated for both cohorts at awake baseline and during xenon administration. *In silico* simulations with two computational models of neurones were performed to investigate how xenon antagonism of hyperpolarisation-activated cyclic nucleotide-gated channel 2 (HCN2) and glutamatergic excitatory neurotransmission would influence peak alpha frequency.
Results: Compared with awake baseline, frontal peak alpha frequency was significantly lower during xenon administration in the randomised controlled trial cohort, median (inter-quartile range) frequency 7.73 Hz (7.27–8.08 Hz) *vs* 8.81 Hz (8.35–9.03 Hz), P=0.012, and the volunteer cohort, 8.69 Hz (8.34–8.98 Hz) *vs* 9.41 Hz (9.11–9.92 Hz), P=0.001. *In silico* simulations with both computational models suggest that antagonism of HCN2 and glutamatergic excitatory neurotransmission are associated with a reduction in peak alpha frequency.
Conclusions: Xenon administration is associated with a reduction of peak alpha frequency in the frontal EEG. *In silico* simulations utilising two computational models of neurones suggest that these changes are consistent with antagonism of HCN2 and glutamatergic excitatory neurotransmission.
Clinical trial registration: The Australian New Zealand Clinical Trials Registry: ANZCTR number 12618000916246.

Keywords: computational modelling; depth of anaesthesia; electroencephalogram modelling; mechanisms of anaesthesia; xenon anaesthesia

One of the most recognisable and widely reported changes in the EEG during conventional propofol or volatile anaesthesia is an increase in frontal alpha oscillation power.[1] More recent investigations have identified that the frequency with the greatest power within the alpha (and upper theta) range, referred to here as the peak alpha frequency (PAF), has a reliable inverse relationship with anaesthetic agent effect-site concentrations.[2,3] A reduction in the PAF has also been identified as a more reliable marker of increasing anaesthetic depth than alpha oscillation power itself.[3] Given the poor correlation between effect-site concentrations of anaesthetic agents and commonly utilised processed EEG indices,[4,5] the

Received: 20 September 2024; **Accepted:** 6 November 2024

PAF might allow for more reliable titration of anaesthetic agents. This is of particular importance for xenon anaesthesia, in which processed EEG indices can significantly overestimate anaesthetic depth.[6,7]

Xenon interacts with a number of membrane-bound ion channels including the excitatory glutamatergic receptors, N-methyl-D-aspartate (NMDA) receptor and α-amino-3-hydroxy-5-methyl-4-isoxazolepropionic acid (AMPA) receptor, and the voltage-gated hyperpolarisation-activated cyclic nucleotide-gated channel 2 (HCN2).[8,9] In contrast to ketamine and nitrous oxide, xenon antagonises both NMDA *and* AMPA receptor-induced currents in electrophysiology studies[8] and blocks long-term potentiation in murine hippocampus.[10] In contrast to other conventional anaesthetic agents, xenon is also devoid of activity at postsynaptic gamma-aminobutyric acid (GABA) receptors.[8,11,12] The novelty of its structure and interactions, compared with other anaesthetic agents, make xenon an ideal agent to study the nature of anaesthetic mechanisms.[13]

Whilst the interactions between anaesthetic agents and membrane-bound ion channels are well described,[8,14,15] general anaesthesia is not a phenomenon observed at the cellular level. Understanding the link between 'micro-level' cellular effects and the observed 'macro-level' network effects that represent general anaesthesia remains a significant challenge.[16]

One validated method for bridging the divide between events at the microscopic cellular level and the macroscopic scale at which biophysical measurements are made is computational modelling of neurones.[17] Such models are based on neurophysiological measurements and their outputs can be directly compared with clinically derived biophysical measurements such as the EEG.

Computational models can be divided into two broad groups, microscopic and mesoscopic.[18] The microscopic approach models neurones and their interactions individually and networks of neurones can be built up from these individual units. However, modelling the interactions of these individual units at a scale relevant to biophysical measurements (thousands of neurones) can become computationally challenging.[17,19]

The second approach emphasises the properties of populations of neurones. Mean field models (MFM) average the responses of populations of neurones across a physiologically relevant scale, from a few millimetres to a few centimetres, and are often described as mesoscopic in scale. By averaging neuronal responses, some of the underlying complexity of interactions within and between neurones can be overlooked whilst the model retains physiological relevance.[17,19]

The highly synchronised alpha oscillations observed during propofol and volatile anaesthesia have been proposed as the mechanism by which these agents disrupt thalamocortical communication.[1,2] Reductions in functional connectivity between the thalamus and cortex have also been described for a wide range of anaesthetic agents.[20] Investigating alpha oscillatory dynamics during xenon anaesthesia (through PAF) might reveal if such changes are limited to anaesthetics with activity at GABA receptors, or if they represent a broader pathway to general anaesthesia.

This study has two aims. The first is to identify if xenon administration is associated with a change in frontal PAF *in vivo*. The second aim is to identify if two reported cellular actions of xenon, antagonism of HCN2 and excitatory glutamatergic receptors, are associated with a reduction in PAF in computational models of neurones. We utilised two models which have previously been used to investigate alpha oscillations during propofol anaesthesia.[21,22]

Methods

Data collection

This study includes a *post hoc* analysis of EEG recordings obtained during administration of xenon gas in two studies. The first was a randomised controlled trial of xenon and sevoflurane anaesthesia in patients scheduled for a minor procedure, performed at St. Vincents Hospital, Melbourne, and approved by the ethics committee at the same institution (approval number HREC/18/SVHM/221) (RCT study). This clinical study was registered with the Australia New Zealand Clinical Trials Registry (ANZCTR number 12618000916246). The second study compared xenon and nitrous oxide gas administration in healthy volunteers, performed at Swinburne University, Melbourne, and approved by the Alfred Hospital and Swinburne University of Technology ethics committee (approval number 260/12) (volunteer study). Results from both studies have previously been published elsewhere alongside detailed descriptions of the methods used.[23–25]

In the RCT study, 24 participants aged >50 yr, were randomly allocated to receive maintenance general anaesthesia with either xenon (end-tidal concentration target 60%) or sevoflurane (0.9 age-adjusted $MAC_{anaesth}$) for extracorporeal shock wave lithotripsy, a procedure with no skin incision. Anaesthesia induction was with propofol 2 mg kg^{-1} and intraoperative analgesia was provided with an infusion of remifentanil 0.1 μg kg^{-1} min^{-1}. The EEG was obtained from the Brain Anaesthesia Response Monitor (BAR, Cortical Dynamics, Perth, Western Australia, Australia), a processed EEG depth of anaesthesia monitor with a proprietary index.[26] The unprocessed EEG from a Fpz/M1 (or M2) montage, with Fp1/2 as ground, was obtained from the BAR at a sampling frequency of 480 Hz.

In the volunteer study, 21 right-handed males aged between 20 and 40 yr received xenon and nitrous oxide via facemask, in a two-way cross-over experimental design with at least 7 days between each gas administration. The xenon gas concentrations administered were 8%, 16%, 24%, and 42% (0.25, 0.5, 0.75, and 1.3 MAC_{awake}).[27] An auditory continual performance task was performed by the participants throughout gas administration to monitor for loss and recovery of responsiveness. In the case of xenon administration at 42%, xenon was delivered until loss of responsiveness and then for a maximum of 10 min after loss of responsiveness. A 64-channel sensor cap (WaveGuard™, Advanced Neuro Technology, Enschede, Netherlands) was utilised to record the EEG which was sampled at 512 Hz. Only the EEG recorded during the administration of xenon 42% (1.3 MAC_{awake}) was included in this analysis.

EEG analysis

EEG data analysis from the RCT and volunteer studies was performed in MATLAB utilising custom scripts. Unprocessed EEG recordings from both studies were band-pass filtered between 0.5 and 45 Hz using the *bandpass.m* function.

Eleven participants received xenon anaesthesia in the RCT study. Significant artifact was present in one EEG recording at the commencement of xenon inhalation and this recording was excluded from further analysis.

Twenty-one EEG recordings were available from the volunteer study. Five participants did not achieve loss of responsiveness during xenon administration because of excessive nausea or gas leakage.[23] Sixteen participants completed the full xenon administration protocol at 42% until loss of responsiveness. From these recordings a frontal montage was created by taking an average of the four frontal channels, Fp1/Fp2 and F7/F8. For this frontal montage, five of the 16 waveforms had significant movement artifact and were excluded from further analysis.

Thus, 10 complete recordings were available for analysis from the RCT cohort and 11 from the volunteer cohort. The characteristics of those participants included in the EEG analysis are presented in Table 1. The spectrograms of all participants, both those included and those excluded from further analysis, are presented in Supplementary Figures S1–S3.

Calculation of frontal peak alpha frequency

A continuous measure of PAF was calculated for both the RCT and the volunteer study frontal EEG recordings by the same method. As noted by previous authors, during both propofol and volatile anaesthetic administration the PAF can transition to values <8 Hz.[3,28] This phenomenon could also be observed in a number of our own EEG recordings and therefore an extended alpha range was utilised (6–12 Hz). The unprocessed EEG signal was band-pass filtered between 6 and 12 Hz. The zero-crossing rate of this band-pass filtered signal (*zerocrossing.m*) was calculated for a 30 s moving window with no overlap. The PAF was then obtained by multiplying the crossing rate by the sampling frequency and dividing that value by two (since there are two zero crossings for each complete oscillation). Example spectrograms and PAF trajectories for one RCT and one volunteer participant are shown in Fig. 1. The PAF trajectories of all included RCT and volunteer participants are presented in the Supplementary Figures S4 and S5.

For the RCT cohort, the PAF for two 30 s periods was compared, 30 s at awake baseline (immediately before propofol induction), and 30 s before cessation of xenon administration.

For the volunteer cohort, the PAF was also calculated for two time periods. The initial 30 s of the recording, at which point there is expected to be little or no xenon effect, was taken as the baseline. This was compared with the PAF during loss of responsiveness (from loss of response until return of response to auditory task). Given the relative brevity of the loss of response period in the volunteer group, the PAF was calculated for the entire loss of response period, as opposed to a 30 s window, to provide a more reliable measure of PAF.

Table 1 Participant characteristics. Characteristics of participants for which peak alpha frequency analysis was performed. Data for age are presented as mean (range). Data for height, weight and body mass index (BMI), are presented as mean (standard deviation). Sex and ASA classification are shown as number (percentage).

	Randomised controlled trial cohort $N=10$	Volunteer cohort $N=11$
Age (yr)	59 (51–72)	28 (22–40)
Height; (cm)	169.8 (7.4)	181.0 (9.7)
Weight; (kg)	76.6 (16.8)	79.5 (14.6)
BMI	26.4 (4.6)	24.3 (3.8)
Sex; (male)	6 (60%)	11 (100%)
ASA; 1	2 (20%)	11 (100%)

Microscopic Hodgkin Huxley model of the thalamus

This model, of 50 thalamocortical (TC) cells and 50 reticular thalamus (RE) cells, was implemented using the open-source MATLAB code provided by Soplata and colleagues[21] (Fig. 2a).

Each individual neurone is a conductance-based single compartment model, originally described by Hodgkin and Huxley,[29] with several 'mechanisms' which represent the time and voltage-sensitive ion channels, and a voltage-insensitive leak channel.[21] The evolution over time of the current through each of these channels is described by a series of second order partial differential equations (see original publication[21] for details). The connections between TC and RE cells are modelled as an AMPA current for excitatory synapses and a GABA current for inhibitory synapses. The AMPA connections have a single parameter for maximal conductance (gAMPA) whilst the GABA connections have two parameters, one for maximal conductance and a second for the time constant of decay.

In this study, we varied three model parameters. The first two parameters are those utilised by Soplata and colleagues[21] to describe a two-dimensional matrix of thalamic activity, based on the maximal conductance of the HCN2 channel of TC cells (gH, units mS cm^{-2}) and the background excitation (I_{app}, units μA cm^{-2}). The background excitation is the initial current applied to both populations of neurones at the outset of each simulation. It is intended as a combined measure of the changes in input into the thalamus from neuromodulators and brainstem excitation that might be reasonably expected during loss of consciousness.

The third parameter we varied, the effects of which have not previously been described, was the AMPA receptor maximal conductance. The ionic currents through both HCN2 and AMPA receptors are reportedly reduced by xenon.[8,9] For the model simulations, we utilised a similar range of physiologically relevant HCN2 conductance values (gH) and background excitation values (I_{app}) as that described by Soplata and colleagues.[21] For each gH and I_{app} combination, we performed a model simulation with two different values of AMPA receptor maximal conductance, the baseline value utilised by Soplata and colleagues[21] (gAMPA 0.08) and 50% of baseline (gAMPA 0.04), intended to model the effect of xenon on AMPA receptor conductance.

The Hodgkin Huxley model (HHM) has several outputs that can be described over time when the equations are computationally solved by Euler's method (with time resolution 0.01 ms). In this study, the outcomes of interest were the membrane potentials of TC and RE cells over a 4000 ms simulation. From these simulations, the firing rate of each population (number of threshold potentials in the final 1000 ms of the simulation) was obtained.

This simulation duration reliably indicated if the modelled cell firing was absent, defined as no threshold potential after the initial activation, transient, no threshold potentials beyond 2000 ms, or sustained, threshold potentials present throughout the 4000 ms window.

Thalamocortical mean field model

This model is the modified Hindricks and van Putten thalamocortical model[22] based on the mean field equations

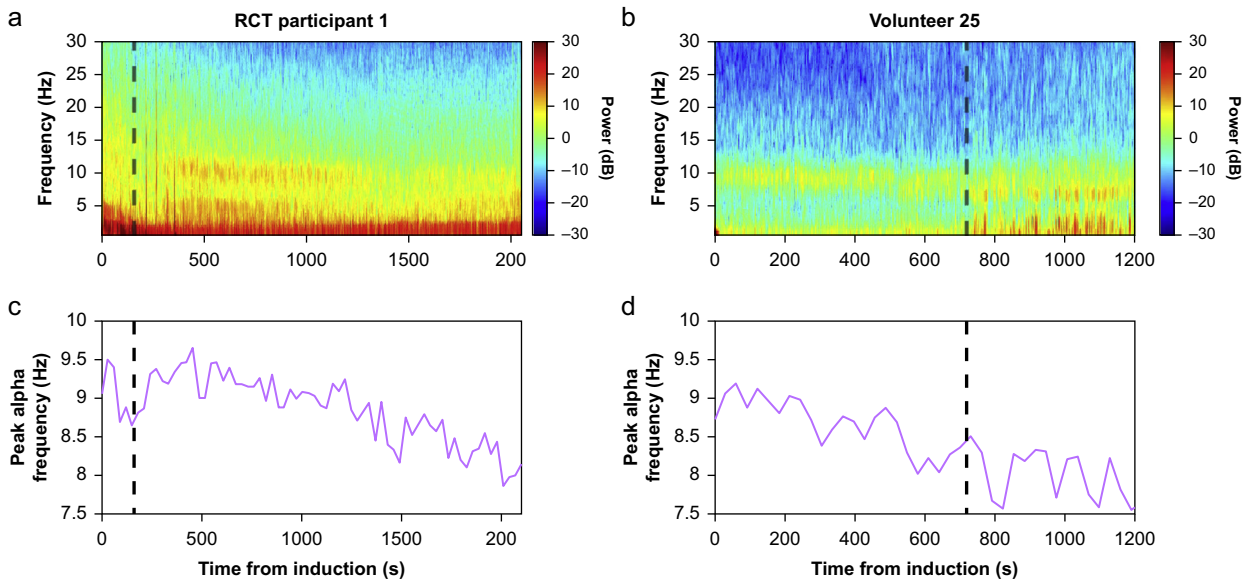

Fig 1. Spectrograms of two participants, one from the randomised controlled trial (RCT) cohort (a) and one from the volunteer cohort (b). Grey dashed line indicates commencement of xenon inhalation in RCT participant, and onset of loss of response in the volunteer cohort. (c, d) Corresponding peak alpha frequency trajectory (30 s windows with no overlap) for the two example spectrograms.

developed by Rennie *et al.*[51] The model describes four populations of neurones, an excitatory and inhibitory thalamic population and an excitatory and inhibitory cortical population (Fig. 2b). All four populations are linked by both excitatory and inhibitory connections. The model was implemented in MATLAB utilising custom scripts (used with permission) originally developed by Alistair and Moira Steyn-Ross (School of Engineering, University of Waikato, New Zealand).

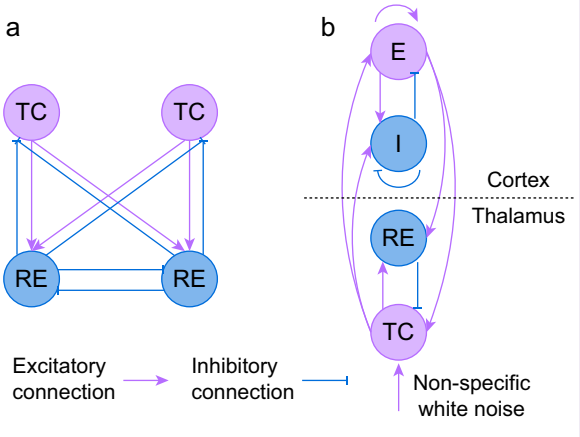

Fig 2. Schematic illustration of the two computational models of neurones utilised. (a) Hodgkin Huxley thalamocortical model. Only two cells of each type shown for simplicity. (b) Mean field model. Long range connections (from thalamus to cortex and vice versa) are subject to a thalamocortical loop delay of 40 ms. E, excitatory pyramidal cortical cell; I, inhibitory cortical cell; RE, reticular thalamus cell; TC, thalamocortical cell. Created with Biorender.com.

The time-varying voltage of a neuronal population's mean membrane potential within the model is the sum of post-synaptic potentials generated in response to afferent connections from other populations. The shape and magnitude of these potentials are scaled and shaped by a synaptic strength and dendritic response function. Long-range excitatory connections (from excitatory thalamic neurones to both cortical neurone populations and excitatory cortical neurones to both thalamic populations) are subject to a thalamocortical loop delay of 40 ms. The firing activity of each population is dependent on a sigmoidal function relating membrane potential to firing rate.

The fluctuation of the membrane potential of the excitatory population around its steady state value, in response to low-intensity white noise which models subthalamic input, provides a voltage time-series. At first approximation, the clinical EEG is a spatially smeared and filtered version of the summed fluctuations of populations of cortical pyramidal neurones. Thus, the voltage time-series of the modelled population of cortical excitatory neurones is termed the 'pseudo-EEG'.

In this study we investigated the effect of varying the excitatory synaptic strength (EXC), a parameter that scales the input from excitatory populations in the model. This parameter determines the excitatory postsynaptic potentials (EPSPs) generated from excitatory inputs. In our simulations, we applied a multiplier to the synaptic strength of all excitatory connections (from both thalamic and cortical excitatory neurones) from 0.5 (50% of baseline EXC) to 1.0 (100% of baseline EXC). The EXC parameter was chosen as there is evidence that xenon antagonises current flow through all subtypes of excitatory glutamatergic receptors.[8] Of note, the EXC is intended to model the effects of xenon on the EPSPs generated

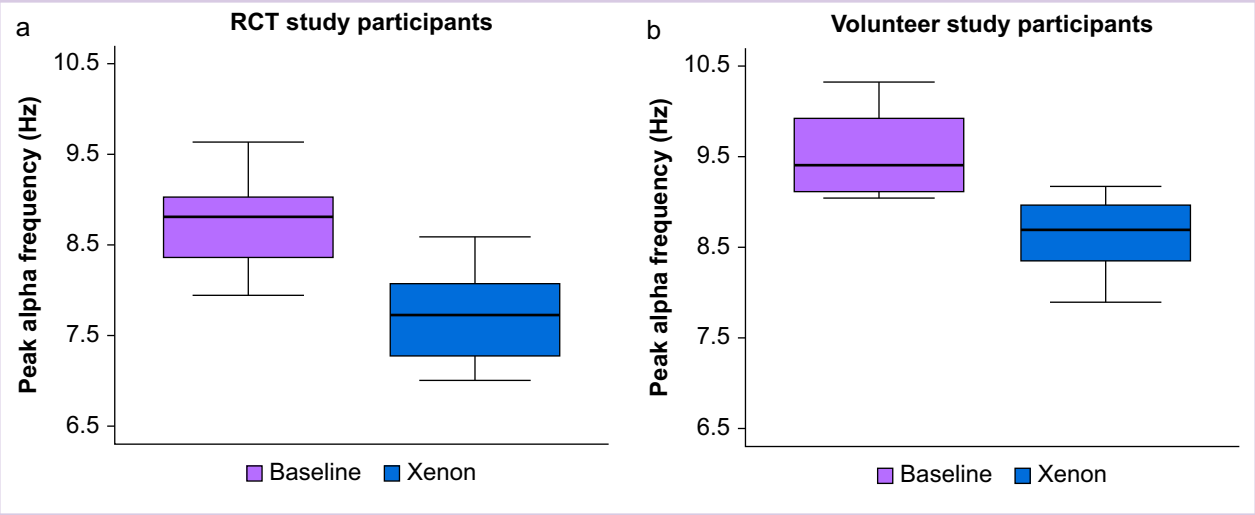

Fig 3. Frontal peak alpha frequency (PAF) at baseline and during xenon-induced loss of consciousness. (a) Randomised controlled trial (RCT study) participants. (b) Volunteer study participants. In both study cohorts, the median PAF was significantly lower during xenon-induced loss of consciousness than at baseline (RCT study, $P=0.012$, volunteer study, $P=0.001$).

by both AMPA and NMDA receptors. This contrasts with the HMM that only models AMPA receptor maximal conductance.

The model operates on three steady state branches, each representing a distinct conscious state, and can transition between these branches (referred to as a state transition). For the purposes of this study, which is focused on understanding general anaesthetic mechanisms, the model was operated on the lower branch only, the steady state branch relevant to the general anaesthetic state.[22]

The output of the model utilised herein was the power spectral density derived from the 'pseudo-EEG'. The PAF was obtained from the power spectral density by identifying the frequency bin, within our extended alpha range of frequencies (6–12 Hz), with the greatest power.

Statistical analysis

This study describes an exploratory analysis of EEG from previous studies and no *a priori* calculation was performed for sample size. Statistical analysis was performed with Stata (Stata/IC 14.2, Stata Corporation, College Station, TX, USA). Non-parametric Wilcoxon signed-rank tests for paired data (significance level $P<0.05$) were utilised to compare the frontal PAF at awake baseline and during xenon administration. Data are expressed as median (inter-quartile range [IQR]).

Results

Changes in frontal PAF associated with xenon administration

In the RCT cohort, the median frontal PAF was significantly lower immediately before ceasing xenon 60% administration, median frequency 7.73 Hz (IQR 7.27–8.08 Hz), than at awake baseline, median frequency 8.81 Hz (IQR 8.35–9.03 Hz) (Fig. 3a, $P=0.012$).

In the volunteer cohort, median frontal PAF was significantly lower during loss of responsiveness with xenon 42%, median frequency 8.69 Hz (IQR 8.34–8.98 Hz) than at awake baseline, median frequency 9.41 Hz (IQR 9.11–9.92 Hz) (Fig. 3b, $P=0.001$).

In silico modelling of the cellular actions of xenon

The results of *in silico* simulation in both models were consistent with the observed EEG effects of xenon administration, namely, a reduction in the PAF.

Effects of altering AMPA receptor maximal conductance on the HHM

In the HMM, sustained firing of TC cells (firing rate >0 in final 1000 ms of simulation) occurred within a confined set of parameters for HCN2 conductance (gH) and background excitation (Fig. 4a). TC firing could occur with or without reciprocal firing of RE cells, although for TC firing rates >4 Hz, reciprocal RE firing was required (Fig. 4c). The parameters that allowed for reciprocal firing were limited to those with a background excitation (≥ 0 μA cm^{-2}) and lower values of HCN2 conductance ($<75\times10^4$ mScm^{-2}).

Reducing AMPA receptor maximal conductance (gAMPA) to 50% of baseline (Fig. 4b and d) had two effects on the TC and RE populations. The first effect was that at equivalent parameters, the firing rate of the TC and RE populations was reduced by around 1–2 Hz when compared with normal connection strength. The second effect was to restrict the region for which there is both reciprocal TC and RE firing. This necessarily limited the parameter space at which higher frequency firing of TC cells was possible.

Effects of reducing excitatory synaptic strength on the MFM

In the MFM, at baseline excitatory synaptic strength (EXC=1), there was power >40 au (arbitrary units) within both the delta and alpha frequency range. As EXC was reduced, the alpha range oscillation was both reduced in power and transitioned to lower frequency bins, indicating a reduction in PAF (Fig. 5).

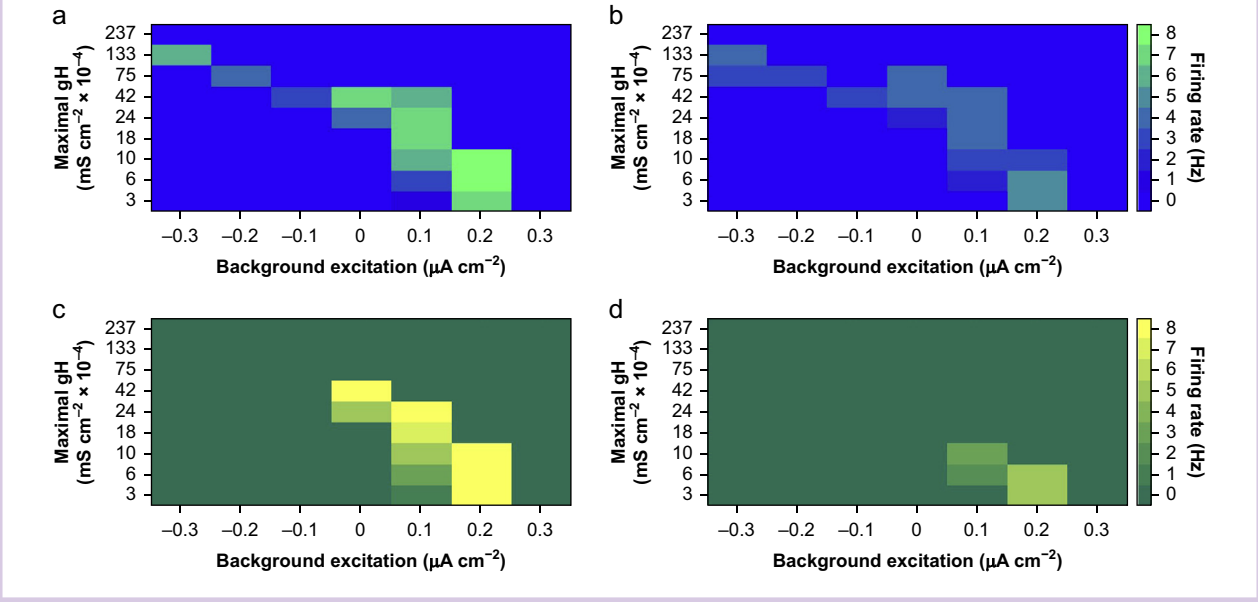

Fig 4. The effects of varying excitatory connection strength (EXC) on the thalamocortical (TC) and reticular thalamus (RE) firing rates (Hz) from Hodgkin Huxley-based thalamic model (HHM). The matrix describes the firing rate across a range of values for background excitation (x-axis) and maximal HCN2 conductance (y-axis). Note that the highest firing rates are associated with lower values of HCN2 maximal conductance (gH). (a) TC firing rate with 100% baseline EXC; (b) TC firing rate with 50% baseline EXC; (c) RE firing rate with 100% baseline EXC; (d) RE firing rate with 50% baseline EXC. Reducing EXC by 50% (b and d) results in a lower firing rate in both TC and RE cells when compared with baseline (a and c). HCN2, hyperpolarisation-activated cyclic nucleotide-gated channel 2.

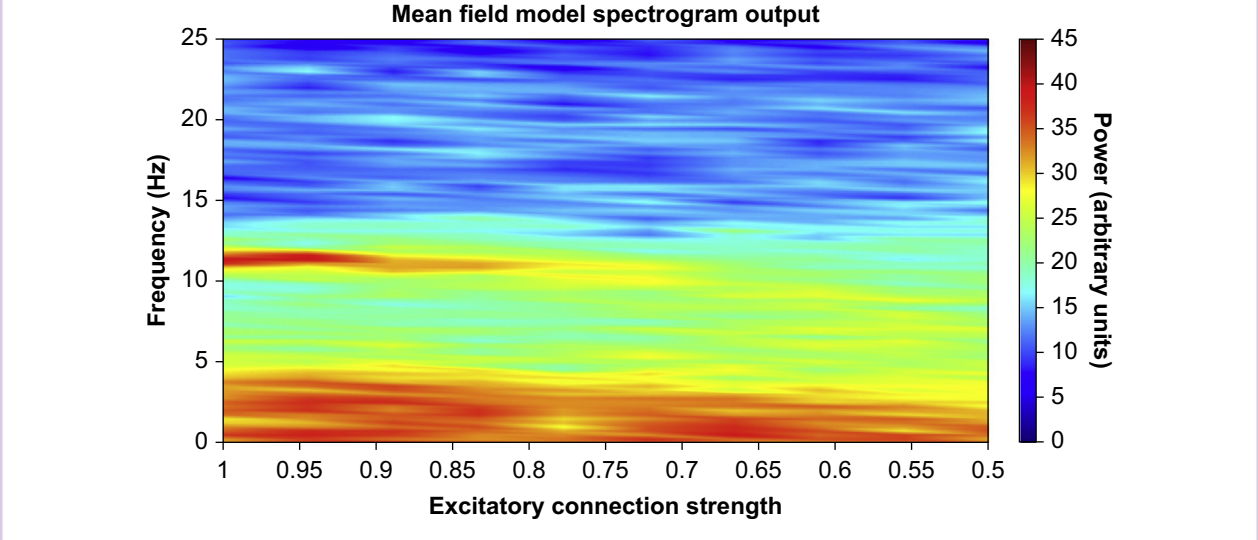

Fig 5. Mean field model output with reducing excitatory connection strength (EXC) presented as a spectrogram. This spectrogram illustrates how the power spectral density of the model output changes as a function of reducing EXC, intended to model the effect of xenon, rather than time (as is the case with a usual spectrogram). Note that as the EXC reduces from 1.0 to 0.7 (moving left to right on x-axis, increasing xenon effect) the peak power in the alpha range moves to lower frequencies (moves down the y-axis) before dissipating.

Discussion

In this study, we identified that the frontal EEG PAF is reduced during xenon administration, and *in silico* simulations with two computational models of neurones indicated that cellular-level actions of xenon are congruent with this observed phenomenon. The former finding has implications for the generalisability of PAF as an indicator of anaesthetic depth and the second finding suggests that disruption of

thalamocortical circuits might be a broader pathway to general anaesthesia than previously understood.

Xenon administration reduces frontal EEG PAF *in vivo*

We observed a reduction in frontal PAF in two participant cohorts administered xenon, an older surgical and a younger volunteer cohort. This consistent reduction in PAF contrasts with the effects of xenon anaesthesia on frontal absolute alpha power, which appear more variable.[25,30]

A previous analysis of the RCT cohort utilised in this study identified that the group median absolute frontal alpha power during xenon anaesthesia was similar to that observed at awake baseline, and significantly less than that observed during sevoflurane anaesthesia.[25] However, within the xenon group, there was also significant inter-individual variation in alpha power (see spectrograms, Supplementary Fig. S1). In contrast to the RCT study, a study of healthy volunteers who inhaled xenon 63% for 2 h identified that mean frontal alpha power increased significantly from baseline.[30]

The varying effects of xenon on alpha power in these two studies could be related to the characteristics of the two cohorts and the well-recognised inverse relationship between age and frontal alpha power.[31] The mean age of participants in the RCT study was 60 yr,[25] compared with the 20–27-yr-old cohort of the volunteer study (no mean provided).[30] Regardless, the substantial variation in alpha power changes described during xenon anaesthesia, and also reported during volatile anaesthesia,[3] suggest that an alternative measure of effect-site concentration, such as PAF, might be more reliable.

Most processed EEG monitors depend on relative power changes in various frequency bands during anaesthesia to calculate their indices.[32] The indices of these monitors correlate poorly with the effect-site concentrations of anaesthetic drugs,[45] and are less reliable when non-GABA receptor potentiating agents are utilised.[6,32,33] PAF is an alternative measure that might allow for better titration of anaesthetic depth[3] and this study with xenon, which is devoid of activity at GABA receptors,[8,12] suggests that PAF is also a measure that might be applicable to a wider range of anaesthetic agents.

Whilst the absolute changes in PAF described in this study are small (around 1 Hz), such changes provide valuable information regarding effect-site concentration and anaesthetic depth. In a previous study of PAF during sevoflurane anaesthesia, a reduction in PAF of 1 Hz was associated with an increased MAC fraction of 0.4.[3] Such an indicator of effect-site concentration would be especially valuable for xenon, as no agent-specific measures of effect-site concentration have been described for this agent to date.

Although we observed a reduction in PAF in both cohorts in this study, direct comparisons between the cohorts should be made with caution. The xenon dose administered to the cohorts was different, 60% *vs* 42%, and the RCT participants also received a low-dose remifentanil infusion (0.1 μg kg^{-1} min^{-1}). During propofol general anaesthesia, low-dose remifentanil was found to decrease delta power and increase alpha power, although no change in PAF was reported.[34] The behavioural endpoint of the two cohorts, general anaesthesia in the RCT cohort and loss of response to auditory stimulus in the volunteer cohort, also differed.

The awake baseline PAF was different between the two cohorts (Fig. 3) and this likely reflects the age of participants. Previous studies have identified that PAF is higher in the resting awake EEG of younger subjects (20–30 yr) when compared with older subjects (65–75 yr).[35] Importantly, regardless of baseline, the PAF was significantly reduced from baseline during xenon administration in both cohorts. Further study is required to identify if the *magnitude* of reduction is similar amongst younger and older participants receiving an equivalent general anaesthetic dose of xenon.

A dose-dependent reduction in frontal PAF is observed during administration of both propofol and volatile agents.[2,3] The reduction in PAF during propofol anaesthesia has been attributed to potentiation of GABA receptors.[21] However, the presence of the same phenomenon during xenon administration, an NMDA receptor antagonist devoid of activity at GABA receptors, suggests that other molecular mechanisms might be responsible for this phenomenon. We explored these alternative mechanisms with two computational models of neurones.

Antagonism of HCN2 and excitatory transmission reduces PAF in computational models of neurones

Computational models of neurones, both microscopic and macroscopic, have successfully reproduced EEG phenomena observed during the administration of propofol, including: anteriorisation of the alpha oscillation,[36] phase amplitude coupling of the alpha and slow-delta oscillations,[21] and a reduction in PAF as the effect-site concentration of propofol increases.[22] The model parameters that are associated with these outputs, principally prolongation of the decay time of the inhibitory postsynaptic potential, support our understanding of how propofol alters conscious state.

One potential shared molecular target of xenon, propofol, and volatiles is HCN2.[37] Xenon has been shown to reduce maximal conductance through the HCN2 channel in voltage clamp recordings of transfected cells and murine tissue slices.[38] This effect is abolished in slices from transgenic mice in which the HCN2 binding site for xenon is mutated to prevent binding.[9] The same HCN2 mutation also reduces the sensitivity of these transgenic mice to the anaesthetic effects of xenon *in vivo*.[9]

Previous work with an HHM of the thalamus suggested that a reduction in HCN2 conductance is effectively a prerequisite for rhythmic TC firing in the upper theta and alpha frequency range.[21] The authors presented simulations which identified that increasing the model parameter for GABA maximal conductance (gGABA) resulted in an initial *increase* in the TC-RE network firing rate. However, with greater values for gGABA, the network firing rate steadily *decreased*.[21]

We have extended these findings by describing how a reduction in AMPA receptor maximal conductance (gAMPA) interacts with reduced HCN2 conductance to alter the model output. Xenon has been shown to reduce current transfer through the AMPA receptor, and other glutamatergic excitatory receptors, in several preclinical studies.[8] We were able to demonstrate that rhythmic firing of TC cells, along with RE cells, could be maintained when gAMPA was reduced by 50%. Crucially, this reciprocal firing of TC and RE cells was only present with low values of maximal HCN2 conductance (gH, Fig. 4). We also demonstrated that the TC firing rate was reduced by 1–2 Hz when gAMPA was reduced to 50% of baseline. The reduction in TC-RE network firing rate after excitatory antagonism appears congruent with the reduction in network firing rate observed with greater values of inhibitory potentiation identified in the earlier description of the model.[21]

We also explored the effect of antagonising excitatory neurotransmission in a second computational model of

neurones, a modified MFM.[22] The MFM has a cortical component, and a thalamic component, and its output, the 'pseudo-EEG,' is more directly comparable to *in vivo* EEG recordings than the HHM.[22] We identified that a reduction in excitatory synaptic strength, from all excitatory neuronal populations within the model, was associated with a reduction in the PAF (and a reduction in alpha oscillation power) (Fig. 5).

In the original description of the model, the authors presented simulations of the MFM with increasing inhibitory synaptic strength.[22] By increasing the inhibitory strength multiplier from 1.4 to 3.0 (intended to represent a sedative dose of propofol increasing to a general anaesthetic dose), there was a progressive reduction in both alpha oscillation frequency and power.[22]

In our RCT cohort, participants received an initial induction dose of propofol followed by the introduction of an anaesthetic dose of xenon within a few minutes. Based on MFM simulations, this might be expected to produce fluctuations in the PAF, as the opposing effects of a reducing propofol effect-site concentration (as the induction dose redistributes) and increasing xenon effect-site concentration coincide (see Supplementary Fig. S6). We identified such fluctuations in several RCT participants (Supplementary Figs S4 and S7).

Inhibition of excitatory transmission and enhancement of inhibitory transmission appear to influence the output of the two models presented here in a similar manner: a reduction in network firing rate in the HMM (with significant inhibitory potentiation) and a reduction in PAF in the MFM.

In vitro experiments support a role for glutamatergic excitatory transmission in the generation of rhythmic oscillations in the thalamus and the ability of glutamate receptor antagonists to modulate thalamic oscillation frequency. Direct injection of the NMDA receptor antagonist AP5 into the reticular nucleus of the thalamus has been shown to change the firing mode of reticular thalamic cells from single spike firing to a rebound bursting mode, albeit in the delta frequency range.[39,40] The effects of ketamine, AP5 (NMDA receptor specific antagonist), and NBXQ (AMPA receptor specific antagonist) on the frequency of alpha spindles (6–11 Hz) recorded in the thalamus of rats have also been reported.[41,42] In one study, the application of ketamine and AP5 both reduced alpha spindles to a delta frequency (around 2 Hz).[41] In another study, application of AP5 and the AMPA receptor-selective antagonist NBXQ, both reduced the spindle firing rate by ~1–2 Hz, whilst a combination of both abolished spindle activity entirely.[42]

Whilst these reports suggest a role for NMDA receptor-mediated effects in mediating thalamic circuit behaviour, it is important to acknowledge that the action of xenon and ketamine on neural circuits is unlikely to be uniform. Whilst both agents antagonise NMDA receptors, ketamine is a non-use-dependent open-channel blocker and xenon is an allosteric competitive antagonist.[8,43,44] The interaction of nitrous oxide is also distinct, being a non-competitive antagonist at NMDA receptors.[45] Whilst ketamine and nitrous oxide are thought to enhance long-term potentiation in the hippocampus, a proposed mechanism for their rapid antidepressant effect,[46] xenon inhibits long-term potentiation in the hippocampus[10] and has been identified as directly inhibiting AMPA receptor-mediated excitatory currents in electrophysiology studies.[8] These differences in cellular action are reflected in the markedly different profiles of the EEG, cerebral blood flow, and cerebral metabolism observed during the administration of xenon, ketamine, and nitrous oxide.[8,23,25]

Modulation of thalamocortical circuits might contribute to xenon general anaesthetic action

A reduction in thalamocortical functional connectivity has been identified during administration of several general anaesthetics[20] and it is hypothesised that highly synchronised alpha oscillations observed during general anaesthesia directly disrupt communication between the thalamus and cortex.[12] Therefore, we propose that the reproduction of alpha oscillations, and changes in PAF observed in the models, are relevant to the mechanism by which xenon alters consciousness and are not simply incidental changes associated with xenon administration. This is supported by *in vivo* studies in which both reduced anaesthetic sensitivity[9] and reduced thalamocortical transmission were observed in HCN2 knockout mice.[38] Our model simulations suggest that xenon supports the generation of alpha oscillations through its antagonism at HCN2, and that it slows the rate of these oscillations through its antagonism of excitatory glutamatergic receptors.

A limitation of this study is that the computational models utilised were not specifically designed to test hypotheses regarding xenon's mechanism of action. The proposed cellular actions of xenon that we investigated, antagonism of HCN2 and glutamatergic excitatory neurotransmission, are key mediators of thalamocortical network behaviour, but we were limited to cellular interactions that could be parameterised in the models.

The HHM modelled all excitatory connections with an AMPA receptor ion channel.[21] This reflects the difficulty in modelling the NMDA receptor at the microscopic scale because of its more complex kinetics which include: voltage sensitivity, differential response to single and spike-train inputs, and sensitivity to glycine and magnesium concentrations.[47] In contrast, the MFM modelled the effect of scaling EPSPs generated by inputs from excitatory populations rather than modelling an individual ion channel.[22] The MFM therefore describes effects on both AMPA and NMDA receptors, although it cannot delineate differential activity of the two channels.

Other cellular actions of xenon such as potentiation of two-pore potassium channels, potassium-adenosine triphosphatase channels, antagonism of nicotinic acetylcholine receptors, and changes to presynaptic release of excitatory neurotransmitters,[8] should be quantitatively tested with original models designed to specifically investigate sites of action for xenon. Specific modelling of the contrasting action of xenon, ketamine, and nitrous oxide at the NMDA receptor might also provide insight into their contrasting effects on cortical activity.

Further study is required to account for the apparent contradiction of a constant xenon dose (60%) delivered in the RCT group, and the progressive reduction in PAF that occurred throughout the anaesthetic episode (see PAF trajectories in Supplementary Fig. S4). This suggests that the reduction in PAF involves a 'slower' mechanism than antagonism of 'fast' AMPA receptor currents.[21] Our MFM simulations suggest that progressive reduction of EPSP magnitude leads to reduced PAF (Fig. 5). Following this explanation, it is plausible that the gradual decrease in PAF could represent slower synaptic and cellular processes, such as alteration in ion channel presentation at the synapse that occur over time, in the presence of a constant concentration of xenon. Although xenon has been identified to block long-term potentiation in murine

hippocampus,[10] the ability of xenon to induce long-term depression, that could account for a progressive reduction in EPSP magnitude without increasing dose, would require confirmation with electrophysiology animal studies.

In terms of the models' structure, the HHM lacks a cortical component, a relevant limitation since both thalamus[1,48] and cortex[49] have been hypothesised as the source of alpha oscillations. The lack of a cortical component renders the model output less directly comparable to the EEG, although the firing rate and mode of TC cells has been reported to directly influence alpha oscillation frequency observed in cortex.[41,42,48]

'Microscopic' models, such as the HHM, with multiple ionic channels, gap junctions, and synaptic interactions can become difficult to parameterise with physiologically relevant values, particularly at scales relevant to biophysical signals (many thousands of neurones).[19] Although they do not model cellular interactions in such granular detail, 'macroscopic' MFM, like that utilised in this study, have the advantage of revealing dynamics at the scale of neuronal populations relevant to biophysical signals.[17] The behaviour of functional networks at even greater scale can be studied utilising network neuroscience approaches. These models of functional units and their connections can be utilised to understand and predict network behaviour, although they can be less relatable to the underlying cellular events and physical networks they represent.[50]

The maximum firing rate of TC cells observed in the HHM was 8 Hz, similar to the maximum firing rate in the absence of GABA receptor potentiation, in previous descriptions of the model.[21] It is not clear if the model's sub-alpha firing rate represents a failure to accurately describe the dynamics between TC and RE cells themselves, or if there is another modulatory influence on frequency not reflected in the model. Regardless, we believe that the relative change in firing rate in response to changes in AMPA receptor conductance is more significant than the absolute values themselves.

In conclusion, we have illustrated that the frontal EEG PAF is reduced, compared with awake baseline, during xenon administration. Monitoring PAF might allow for better titration of a wider range of general anaesthetic agents than conventional processed EEG indices. Reduction in PAF appears to be a neurophysiological mechanism shared by xenon, an NMDA receptor antagonist devoid of activity at GABA receptors, and conventional GABA receptor-potentiating anaesthetic agents. We have illustrated that a reduction in PAF can be reproduced in computational models of neurones by antagonism of HCN2 and excitatory neurotransmission, both of which are reported actions of xenon at the cellular level.

Author's contributions

Designed the clinical study, involved in data collection for the volunteer study, performed the data analysis, and modelling and wrote the first draft of the manuscript: SM
Designed and collected data for the volunteer study and reviewed the manuscript: AP
Involved in the design and data collection for the clinical study: DAS
Reviewed the manuscript: DAS, JS
Advised on data analysis and modelling: JS

Declarations of interest

The authors declare that they no conflicts of interest.

Acknowledgements

The authors would like to acknowledge the contributions of Dr Elie Adam (Picower Institute of Learning and Memory, Massachusetts Institute of Technology) for assistance with the electroencephalogram signal analysis and advising on the manuscript and Professor David Liley (Department of Medicine, University of Melbourne) for advising on the manuscript. The authors would also like to acknowledge Alistair and Moira Steyn-Ross (School of Engineering, University of Waikato, New Zealand) for providing the scripts for the mean field model.

Funding

The electroencephalogram data for this study were obtained from two studies which were supported by grants from The ANZCA Research Foundation, Australian and New Zealand College of Anaesthetists (N20/009) and a James S. McDonnell Foundation collaborative grant (220020419).

Appendix A. Supplementary data

Supplementary data to this article can be found online at https://doi.org/10.1016/j.bjao.2024.100358.

References

1. Purdon PL, Sampson A, Pavone KJ, Brown EN. Clinical electroencephalography for anesthesiologists: Part I: background and basic signatures. *Anesthesiology* 2015; **123**: 937–60
2. Purdon PL, Pierce ET, Mukamel EA, et al. Electroencephalogram signatures of loss and recovery of consciousness from propofol. *Proc Natl Acad Sci U S A* 2013; **110**: E1142–51
3. Hight D, Voss LJ, Garcia PS, Sleigh J. Changes in alpha frequency and power of the electroencephalogram during volatile-based general anesthesia. *Front Syst Neurosci* 2017; **11**: 36
4. Whitlock EL, Villafranca AJ, Lin N, et al. Relationship between bispectral index values and volatile anesthetic concentrations during the maintenance phase of anesthesia in the B-Unaware trial. *Anesthesiology* 2011; **115**: 1209–18
5. Schnider TW, Minto CF, Filipovic M. The drug titration paradox: correlation of more drug with less effect in clinical data. *Clin Pharmacol Ther* 2021; **110**: 401–8
6. McGuigan S, Scott DA, Evered L, Silbert B, Liley DTJ. Performance of the bispectral index and electroencephalograph derived parameters of anesthetic depth during emergence from xenon and sevoflurane anesthesia. *J Clin Monit Comput* 2023; **37**: 71–81
7. Fahlenkamp AV, Krebber F, Rex S, et al. Bispectral index monitoring during balanced xenon or sevoflurane anaesthesia in elderly patients. *Eur J Anaesthesiol* 2010; **27**: 906–11
8. McGuigan S, Marie DJ, O'Bryan LJ, et al. The cellular mechanisms associated with the anesthetic and neuroprotective properties of xenon: a systematic review of the preclinical literature. *Front Neurosci* 2023; **17**, 1225191
9. Kassab NED, Mehlfeld V, Kass J, Biel M, Schneider G, Rammes G. Xenon's sedative effect is mediated by interaction with the cyclic nucleotide-binding domain (CNBD) of HCN2 channels expressed by thalamocortical neurons

of the ventrobasal nucleus in mice. Int J Mol Sci 2023;24: 8613
10. Kratzer S, Mattusch C, Kochs E, Eder M, Haseneder R, Rammes G. Xenon attenuates hippocampal long-term potentiation by diminishing synaptic and extrasynaptic N-methyl-D-aspartate receptor currents. *Anesthesiology* 2012; **116**: 673–82
11. Franks NP, Dickinson R, de Sousa SL, Hall AC, Lieb WR. How does xenon produce anaesthesia? *Nature* 1998; **396**: 324
12. de Sousa SL, Dickinson R, Lieb WR, Franks NP. Contrasting synaptic actions of the inhalational general anesthetics isoflurane and xenon. *Anesthesiology* 2000; **92**: 1055–66
13. Roose BW, Zemerov SD, Dmochowski IJ. Xenon-protein interactions: characterization by X-ray crystallography and hyper-CEST NMR. *Methods Enzymol* 2018; **602**: 249–72
14. Chau PL. New insights into the molecular mechanisms of general anaesthetics. *Br J Pharmacol* 2010; **161**: 288–307
15. Lambert DG. Mechanisms of action of general anaesthetic drugs. *Anaesth Intensive Care Med* 2020; **21**: 235–7
16. Mashour GA, Sanders RD, Lee U. Propofol anesthesia: a leap into the void? *Anesthesiology* 2022; **136**: 405–7
17. Carlu M, Chehab O, Dalla Porta L, et al. A mean-field approach to the dynamics of networks of complex neurons, from nonlinear Integrate-and-Fire to Hodgkin–Huxley models. *J Neurophysiol* 2020; **123**: 1042–51
18. Evertz R, Hicks DG, Liley DT. Alpha blocking and 1/fβ spectral scaling in resting EEG can be accounted for by a sum of damped alpha band oscillatory processes. *PLoS Comput Biol* 2022; **18**, e1010012
19. Coombes S, beim Graben P, Potthast R, Wright J. *Neural fields: theory and applications*. Berlin, Heidelberg: Springer; 2014
20. Hemmings HC, Riegelhaupt PM, Kelz MB, et al. Towards a comprehensive understanding of anesthetic mechanisms of action: a decade of discovery. *Trends Pharmacol Sci* 2019; **40**: 464–81
21. Soplata AE, McCarthy MM, Sherfey J, et al. Thalamocortical control of propofol phase-amplitude coupling. *PLoS Comput Biol* 2017; **13**, e1005879
22. Noroozbabaee L, Steyn-Ross DA, Steyn-Ross ML, Sleigh JW. Analysis of the Hindriks and van Putten model for propofol anesthesia: limitations and extensions. *NeuroImage* 2021; **227**, 117633
23. Pelentritou A, Kuhlmann L, Cormack J, et al. Source-level cortical power changes for xenon and nitrous oxide-induced reductions in consciousness in healthy male volunteers. *Anesthesiology* 2020; **132**: 1017–33
24. McGuigan S, Evered L, Scott D, Silbert B, Zetterberg H, Blennow K. Comparing the effect of xenon and sevoflurane anesthesia on postoperative neural injury biomarkers: a randomized controlled trial. *Med Gas Res* 2022; **12**: 10–7
25. McGuigan S, Evered L, Silbert B, et al. Comparison of the spectral features of the frontal electroencephalogram in patients receiving xenon and sevoflurane general anesthesia. *Anesth Analg* 2021; **133**: 1269–79
26. Liley DT, Sinclair NC, Lipping T, Heyse B, Vereecke HE, Struys MM. Propofol and remifentanil differentially modulate frontal electroencephalographic activity. *Anesthesiology* 2010; **113**: 292–304
27. Goto T, Nakata Y, Saito H, et al. Bispectral analysis of the electroencephalogram does not predict responsiveness to verbal command in patients emerging from xenon anaesthesia. *Br J Anaesth* 2000; **85**: 359–63
28. Hindriks R, van Putten MJAM. Meanfield modeling of propofol-induced changes in spontaneous EEG rhythms. *NeuroImage* 2012; **60**: 2323–34
29. Hodgkin AL, Huxley AF. A quantitative description of membrane current and its application to conduction and excitation in nerve. *J Physiol* 1952; **117**: 500
30. Laitio RM, Kaskinoro K, Sarkela MO, et al. Bispectral index, entropy, and quantitative electroencephalogram during single-agent xenon anesthesia. *Anesthesiology* 2008; **108**: 63–70
31. Purdon PL, Pavone KJ, Akeju O, et al. The ageing brain: age-dependent changes in the electroencephalogram during propofol and sevoflurane general anaesthesia. *Br J Anaesth* 2015; **115**: i46–57
32. Fahy BG, Chau DF. The technology of processed electroencephalogram monitoring devices for assessment of depth of anesthesia. *Anesth Analg* 2018; **126**: 111–7
33. Hirota K. Special cases: ketamine, nitrous oxide and xenon. *Best Pract Res Clin Anaesthesiol* 2006; **20**: 69–79
34. Kortelainen J, Koskinen M, Mustola S, Seppänen T. Effects of remifentanil on the spectrum and quantitative parameters of electroencephalogram in propofol anesthesia. *Anesthesiology* 2009; **111**: 574–83
35. Jabès A, Klencklen G, Ruggeri P, Antonietti J-P, Banta Lavenex P, Lavenex P. Age-related differences in resting-state EEG and allocentric spatial working memory performance. *Front Aging Neurosci* 2021; **13**, 704362
36. Vijayan S, Ching S, Purdon PL, Brown EN, Kopell NJ. Thalamocortical mechanisms for the anteriorization of alpha rhythms during propofol-induced unconsciousness. *J Neurosci* 2013; **33**: 11070–5
37. Ying S-W, Abbas SY, Harrison NL, Goldstein PA. Propofol block of I(h) contributes to the suppression of neuronal excitability and rhythmic burst firing in thalamocortical neurons. *Eur J Neurosci* 2006; **23**: 465–80
38. Mattusch C, Kratzer S, Buerge M, et al. Impact of hyperpolarization-activated, cyclic nucleotide-gated cation channel type 2 for the xenon-mediated anesthetic effect: evidence from in vitro and in vivo experiments. *Anesthesiology* 2015; **122**: 1047–59
39. Zhang Y, Llinas RR, Lisman J. Inhibition of NMDARs in the nucleus reticularis of the thalamus produces delta frequency bursting. *Front Neural Circuits* 2009; **3**: 20
40. Zhang Y, Buonanno A, Vertes RP, Hoover WB, Lisman JE. NR2C in the thalamic reticular nucleus; effects of the NR2C knockout. *PLoS One* 2012; **7**, e41908
41. Buzsáki G. The thalamic clock: emergent network properties. *Neuroscience* 1991; **41**: 351–64
42. Jacobsen RB, Ulrich D, Huguenard JR. GABAB and NMDA receptors contribute to spindle-like oscillations in rat thalamus in vitro. *J Neurophysiol* 2001; **86**: 1365–75
43. Zhang Y, Ye F, Zhang T, et al. Structural basis of ketamine action on human NMDA receptors. *Nature* 2021; **596**: 301–5
44. Armstrong SP, Banks PJ, McKitrick TJ, et al. Identification of two mutations (F758W and F758Y) in the N-methyl-D-aspartate receptor glycine-binding site that selectively prevent competitive inhibition by xenon without affecting glycine binding. *Anesthesiology* 2012; **117**: 38–47
45. Sanders RD, Weimann J, Maze M, Warner DS, Warner MA. Biologic effects of nitrous oxide: a mechanistic and toxicologic review. *Anesthesiology* 2008; **109**: 707–22

46. Izumi Y, Hsu F-F, Conway CR, Nagele P, Mennerick SJ, Zorumski CF. Nitrous oxide, a rapid antidepressant, has ketamine-like effects on excitatory transmission in the adult hippocampus. *Biol Psychiatry* 2022; **92**: 964–72
47. Iacobucci GJ, Popescu GK. NMDA receptors: linking physiological output to biophysical operation. *Nat Rev Neurosci* 2017; **18**: 236–49
48. Ching S, Cimenser A, Purdon PL, Brown EN, Kopell NJ. Thalamocortical model for a propofol-induced α-rhythm associated with loss of consciousness. *Proc Natl Acad Sci U S A* 2010; **107**: 22665–70
49. Hartoyo A, Cadusch PJ, Liley DT, Hicks DG. Inferring a simple mechanism for alpha-blocking by fitting a neural population model to EEG spectra. *PLoS Comput Biol* 2020; **16**, e1007662
50. Bassett DS, Zurn P, Gold JI. On the nature and use of models in network neuroscience. *Nat Rev Neurosci* 2018; **19**: 566–78
51. Rennie CJ, Robinson PA, Wright JJ. Unified neurophysical model of EEG spectra and evoked potentials. *Biol Cybern* 2002; **86**(6): 457–71

Handling editor: Phil Hopkins